León 05
CIE Midterm Meeting y
Congreso Internacional de Iluminación

CIE

Título del trabajo
Title of paper

Study on Motion Vectors of Video Images under Cybersickness for Visual Image Safety

Autor/ es
Author/s

Tohru Kiryu[1, 3], Eri Nomura[1], Michihiro Kobayashi[1], Atsuhik Iijima[2, 3], and Takehiko Bando[2]

Afiliación/ es del autor/ es
Affiliation/s of the author/s

[1]Graduate School of Science and Technology, Niigata University
[2]Graduate School of Medical and Dental Sciences, Niigata University
[3]Center for Transdisciplinary Research, Niigata University

Dirección principal
Mail adress

8050 Ikarashi 2-nocho, Niigata, 950-2181 Japan

Teléfono, fax. e-mail de la persona de contacto
Phone, Fax number and e-mail adress of the contact person

Phone: +81 25 262 6756, Fax: +81 25 262 7398
e-mail: kiryu@bc.niigata-u.ac.jp

Abstract

Aiming at the suppression of visually induced sickness (cybersicknes) for visual image safety, we are investigating the influences of vection-induced video images on the autonomic regulation quantitatively. Cybersickness is related to factors in both video images and conditions of users. We used the motion vectors to quantify video image scenes and measured electrocardiogram, blood pressure, and respiration for evaluating the autonomic regulation.

The cybersickness intervals were extracted based on the conditions of autonomic nervous activity related indices (low-frequency (LF) and high-frequency (HF) components of biosignals). Then, we determined the triggered onsets that could emerge unpleasant sensation, tracing the time-series of the LF component backwards in time to find out the local minimum. Around the triggered onsets we investigated the features of time-frequency structure of motion vectors by the continuous wavelet transform. Then, we tried to predict the influence of vection-induced video images by system identification with the motion vectors as input signals and the autonomic nervous activity related signals as output signals. We estimated the respiratory sinus arrhythmia (RSA) and the Mayer wave (MW) as autonomic nervous activity related signals. The relationship between motion vectors and RSA or MW was approximated by the linear time-invariant models.

The results showed that a specific time-frequency structure of motion vectors around the triggered onsets would induce sickness. The time-frequency structure of motion vectors generally includes temporal frequencies ranging from 3 to 10 Hz. The time-frequency structure around the triggered onsets was different from the time-frequency structures around weak-cybersickness intervals. Furthermore, the ARX model of MATLAB successfully predicted RSA and MW several seconds ahead. Hence, the potential cybersickness intervals could be estimated by the time-frequency structure of motion vectors. This approach would be helpful for designing the suppression of cybersickenss for each individual.

Keyword: cybersickness, motion vector, biosignals, system identification, ARX model

I. INTRODUCTION

Development of digital imaging technology by computer graphics is producing many image formats, resolutions, frame rates, in addition to conventional factors such as screen sizes, brightness, colors, and display devises. Contrary to the benefits, digital imaging technology is widely spreading unexpected visual stimulus. For example, handy cameras produce unexpected off-centering images. Practical problems are emerging especially in the application of virtual reality (VR) or the virtual environment (VE) to bioengineering regarding telemedicine or rehabilitation. Hence, there are some problems in visual safety in relation to unpleasant sensation and after effects due to visual stimulus. It has been reported that the mismatch between visual system and vestibular system causes sickness (sensory conflict theory) [1]. In 2002, Nichols *et al.* [2] has pointed out health and safety implications of VR to make

recommendations regarding the future direction of VR. However, details in relation to sickness have been still unknown.

Unpleasant sensation has been assessed by autonomic nervous activity related indices estimated from biosignals including heart rate, blood pressure, finger pulse volume, respiration rate, skin condition, and gastric myoelectrical activity. In this paper, we measured electrocardiogram (ECG), blood pressure, and respiration, while watching vection-induced image videos. We quantified vection-induced images by the motion vectors that are used in image data compression. As a similar parameter, So *et al.* tried to propose a metric for quantifying virtual scene movement by the spatial velocity of computer graphic images [3]. The motion vector has superiority in terms of wide applicability for all types of images and also convenience for surveying digital images. Since biosignals and motion vectors were available as a function of time, we analyzed them by the time-frequency representations, and investigated the relationship between the autonomic responses and the motion vector components. Then, we tried to predict the influence of vection-induced video images by system identification with the motion vectors as input signals and the autonomic nervous activity related signals as output signals.

II. METHODS

A. Experiments

Healthy young 22 male and three female subjects (22.4 ± 1.0 yrs. old) participated in the experiments. The subjects were informed of the risks involved in advance, and their ECG, blood pressure, and respiration were monitored at the posture of sitting down in the chair during the experiments. The ECG was measured on the chest and the continuous blood pressure was measured by a tonometry method. The respiration was measured with sensors around the chest and the abdomen. These biosignals were sampled at the rate of 1000 Hz with a 12-bit resolution and stored into a hard disk of a PC. The image was back-projected on an 80-inch screen by the video projectors with XGA and over 2500 ANSI lumen. The distance between a subject and the screen was 2-meters and the illumination was 10 lux.

For the 18-min length vection-induced visual tasks, eleven sessions of different sports experiencing video images: for example, the video camera attached at the top of the mountain bike handle took a down hill scene in the field and it sometimes produced

unexpected camera work. After screening by a simple questioner (unpleasant, nutral, or not), we selected the image of mountain bike session that caused typical cybersickness for almost all the subjects and the image of bobsleigh session that did not always cause cybersickness.

B. Quantification of Images by Motion Vectors

We quantized the video image by the motion vectors (Fig. 1) [4]. We estimated a local motion vector (LMV) by the block matching method in each section of a screen for the image size of 352×288 pixels. Note that the whole image was divided into 25 (5×5) sections. Besides, a global motion vector (GMV), which represents camera work, was estimated from LMV by a bottom-up approach [5]. Each coefficient is easily calculated with the differentiation and clustering procedure.

Using a frame-by-frame sliding window with a 1-sec interval, we estimated the time-series of the correlation coefficients, γ, between three GMV components (zoom, pan, and tilt) and each LMV components (up/down and right/left) at 25 sections in a screen. Moreover, the time-varying behavior of each GMV component was analyzed by the continuous wavelet transform (CWT) as a time-frequency representation.

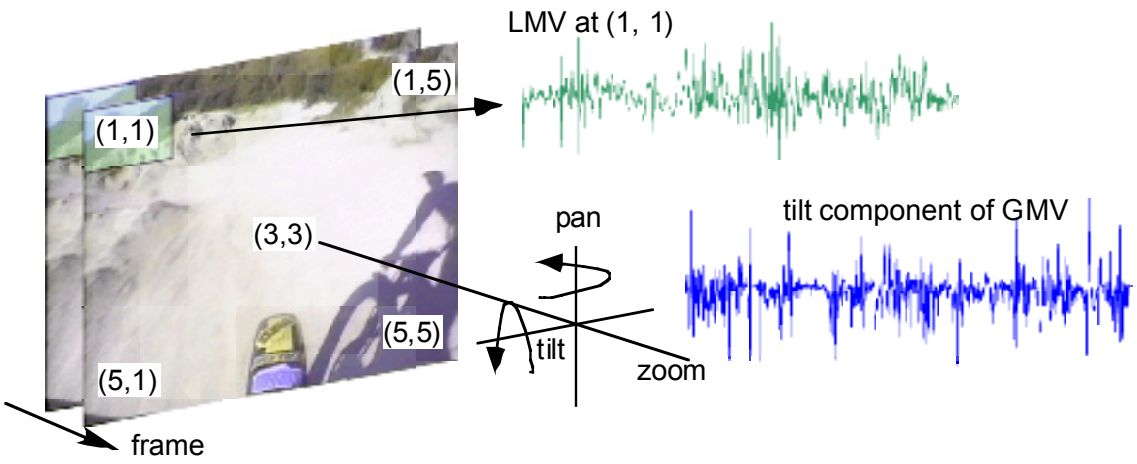

Figure 1. Estimation of motion vectors

C. *Biosignal Processing*

The sampling rate of biosignals was adjusted to the frame rate of images. Since the frame rate was 30 frames/sec, we uniformly resampled interpolated R-R interval time-series at the frequency of 30 Hz. In extraction of autonomic nervous activity (ANA) related indices, the limited frequency rages are 0.04–0.15 Hz for blood pressure and R-R interval (Mayer wave (MW) related signal), and 0.16–0.45 Hz for respiration

and R-R interval (respiratory sinus arrhythmia (RSA) related signal) [6]. Then, we obtained the time-series of the ANA related indices every frame with a 10-sec interval.

After estimating the averaged low-frequency (LF) and high-frequency (HF) power components during each image session for individual subjects, we determined the cybersickness intervals based on the following ANA related conditions [7]: the LF power component is greater than the 120% of averaged LF power component, LF120, and the HF power component is less than the 80% of averaged HF power component, HF80. In addition to the cybersickness intervals, we determined the triggered onsets that could emerge unpleasant sensation, tracing the time-series of the LF power component followed by a cybersickness interval backwards in time and locating a triggered onset as a local minimum of the power. Around the triggered onsets we investigated the features of time-frequency structure of GMVs by the CWT with the Gabor function. That is, we estimated the powers of GMV components at 31 frequency bands for 0.01–15 Hz.

To trace the similar time-frequency structure of GMVs in the local time of each session, we used the similarity function given by

$$\zeta = \cos^2\theta = \left[\frac{(\boldsymbol{g}_0 \cdot \boldsymbol{g})}{\|\boldsymbol{g}_0\| \cdot \|\boldsymbol{g}\|}\right]^2 .$$

The similarity function is presented by a squared cosine function between an arbitrary power vector, $\boldsymbol{g}$, and a reference power vector, $\boldsymbol{g}_0$. The reference power vector was composed of the powers of GMVs averaged around trigger points over 3-sec. The components of the arbitrary power vector were the powers over other 3-sec intervals. The time-series of the similarity was estimated by sliding the 3-sec interval by 1-sec.

D. System Identification Approach

Since GMV as the input and ANA related indices as the output were available, we further executed the system identification approach by the multivariable autoregressive extra input (ARX) model, using motion vectors and MW related signal (Fig. 2). Note that the number of inputs was 3 and the order of the polynomials was 2.

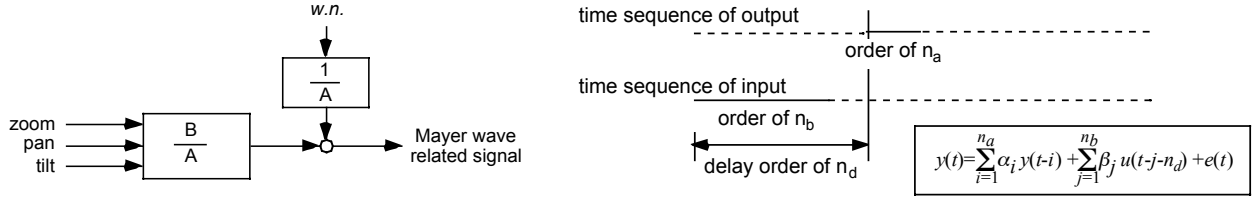

Fig. 2. System function approach for virtual motion.

III. RESULTS

A. Vection-Induced Images analyzed by Motion Vectors

In the mountain bike session $|\gamma| > 0.8$ was located at the center and distant views for both the pan-(right/left) components and the tilt-(up/down) components, whereas $|\gamma|$ was low at the near view (**Fig. 3(a)**). Moreover, the intervals with high $|\gamma|$ were relatively long around 0–10 sec, 40–65 sec, and 90–105 sec in the mountain bike session. The zoom components did not present significant correlation with LMV component except for zoom-(up/down) components around the above intervals at the distant view. On the other hand, in the scene of the bobsleigh session, the high-$|\gamma|$-region distributed in time for the combination of pan-(right/left) components, whereas $|\gamma|$ was low at everywhere for other components (**Fig. 3(b)**).

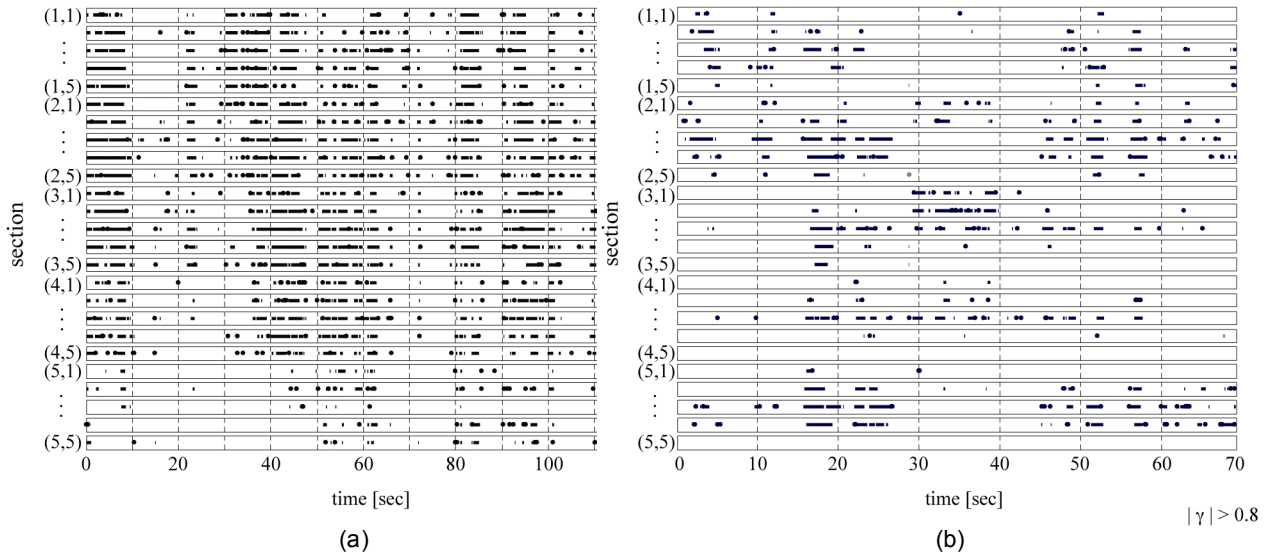

Figure 3. high-$|\gamma|$-region in time and screen

B. Time-Distribution of Trigger Points

We used two pairs of ANA related indices, (LF120, HF80), for determining the cybersickness intervals: LF120 and HF80 estimated from R-R interval, and HF80 from respiration and LF120 from blood pressure. **Figure 4** shows the time-distribution of 36 trigger points for 25 subjects at each 10-sec segment in the mountain bike session. The result showed that the cybersickness intervals were around 61–70 sec and 91–100 sec segments and the time-distribution of the trigger points showed two peaks around these segments. Note that the two peaks were located around the high-$|\gamma|$-regions.

On the other hand, there were 12 trigger points in the bobsleigh session and the time-distribution did not match the high-| γ |-regions.

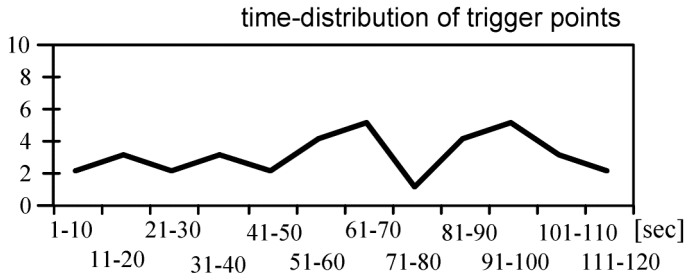

Figure 4. Time-distribution of trigger points

C. Time-Frequency Structure of Motion Vectors in relation to Cybersickness

Checking the details of the time-frequency structure of GMVs over 0.5 in the normalized power around trigger points, the time-frequency structure included low frequencies ranging 0.3–2.5 Hz in three components. Regarding the bobsleigh session, the time-frequency structure included 0.2–5 Hz in the zoom component and 4–11 Hz in the pan and tilt components.

Figure 5 shows the time-varying behavior of the similarity function referring to the two trigger points, 65–68 and 91–94 sec, estimated in the mountain bike session. The similarity showed 1.0 at the trigger points, and decreased around 30 and 80 sec where there was no camera motion (see Figs. 3 and 4). As a result, the overall behavior of the similarity based on the time-frequency structure of GMVs was quite similar to the time-distribution of trigger points estimated from biosignals (see Fig. 3). On the other hand, the overall behavior of the similarity function was not similar to the time-distribution of trigger points in the bobsleigh session.

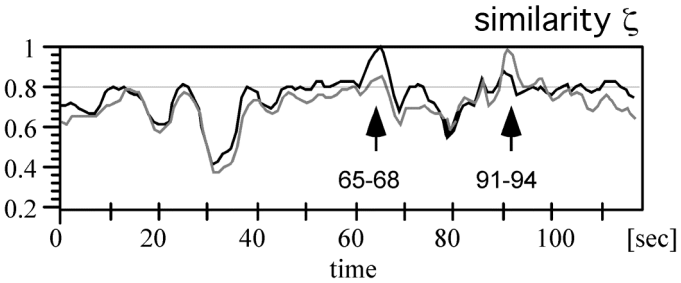

Figure 5. Time-varying behavior of the similarity function referring to the trigger points

Figure 6 demonstrates the results by the system identification approach. From the first half of the mountain bike session, we estimated the parameters of ARX model from (a) the Mayer wave related power and the GMV components: zoom, pan, and tilt. Moreover, we applied these parameters to other session, the bike race session in (b), and successfully estimated the Mayer wave related signal.

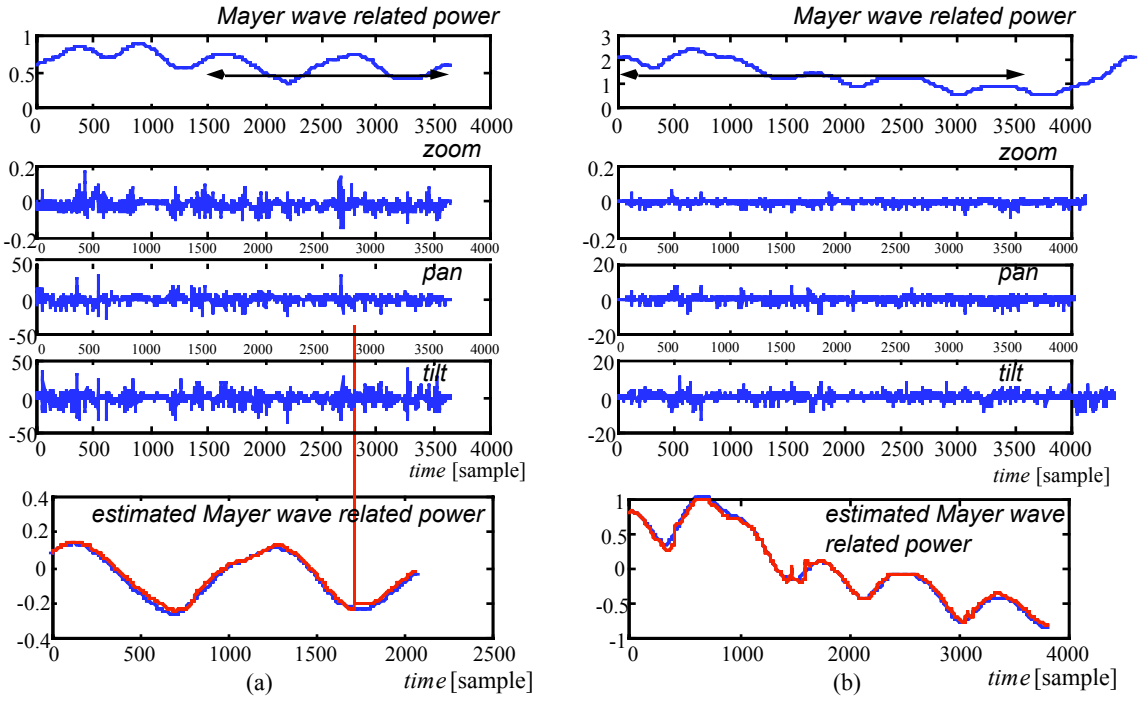

Figure 6. System identification approach

IV. Discussion

A. Characterization of Vection-Induced Images by Motion Vectors

According to the time-series of the correlation coefficients between LMV components at each section and three GMV components, we were able to recognize a region where in the screen and when in the local time of a session the camera work was highlighted. The mountain bike session, the highest cybersickness score of the questionnaire, explicitly had large high-| γ |-regions at the center and distant views in the screen and at limited intervals in the local time (Fig. 2). On the other hand, in the bobsleigh session with lower cybersickness scores, the high-| γ |-regions distributed in the screen and in the local time. The three sessions with the high-| γ |-regions induced

vection, but the specific distribution of high-| γ |-regions in the mountain bike session possibly caused cybersickness.

C. Time-Frequency Structure of Motion Vectors causing Cybersickness

The influences of vection-induced images were caused by many different factors. One of the factors is the video content which evokes the feeling of individual experience. When camera work is hard to be purchased, subjects usually feel unpleasant sensation. Thus, for example, off-centered vection-induced images with certain exposure time intervals could enlarge the sensory conflict [8] and in turn would disturb the autonomic nervous regulation [9], [10].

Referring to the experimental results, the GMV components with the specific frequency bands around 0.3–2.5 Hz affected the autonomic nervous regulation. Although there are differences between cybersickness and motion sickness, it was reported that a motion sickness enlarges under 0.5 Hz of horizontal translational oscillation [11]. The motion vectors alone do not present all of the features, but the time-frequency representation of GMVs allowed us to expect the candidates that would possibly cause cybersickness.

V. CONCLUSION

Preventing cybersickness becomes a key point to apply virtual reality to the variety of potential fields for a long time use. Cybersickness is related to factors in both images and conditions of users. We studied the influences of vection-induced images in the relationships between the autonomic nervous activity related indices and the motion vectors of images.

We determined cybersickenss intervals and the trigger points and compared them with the results based on the motion vectors. Comparing strong cybersickness-induced images with weak cybersicknes-induced images, we concluded that the correlation coefficient between local and global motion vectors represented the potential cybersickness regions in the screen and time, and the time-frequency structure of global motion vectors could be used for expecting the time-distribution of potential trigger points. According to the time-varying behavior of motion vectors, the specific frequency bands around 0.3–2.5 Hz were possibly triggering cybersickness. Hence the high-| γ |-region and the similarity function were superior to others in term of

the special distribution in the screen and the time-distribution in the local time, respectively.

ACKNOWLEDGEMENTS

This study is carried out under the Standard Authentication R&D Program, "Standardization of Assessment Method for Visual Image Safety," promoted by the Ministry of Economy, Trade and Industry in Japan.

REFERENCES

[1] L. J. Hettinger, K. S. Berbaum, R. S. Kennedy, W. P. Dunlap, and M. D. Nolan, "Vection and simulator sickness," *Mil. Psychol.*, vol. 2, no. 3, pp. 171-181, 1990.

[2] S. Nichols and H. Patel, “Health and safety implications of virtual reality: a review of empirical evidence,” *Appl. Ergon.*, vol. 33, no. 3, pp. 251-271, 2002.

[3] R. H. So, A. Ho, and W. T. Lo, “A metric to quantify virtual scene movement for the study of cybersickness: Definition, implementation, and verification,” *Presence*, vol. 10, no. 2, pp. 192-215, 2001

[4] T. Kiryu, Y. Nanbo, N. Kobayasi, and T. Bando, “Relationship between Motion Vectors of Vection-Induced Image and Multivariate Biosignals under Visual Tasks,” in *Proc. 4th International Workshop on Biosignal Interpretation*, pp. 517-520, Como, Italy, 2002.

[5] K. Jinzenji, H. Watanabe, and N. Kobayashi, Global motion estimation for static sprite production and its application to video coding, *IEEE ISPAC’98*, pp. 328-332, 1998.

[6] J. Hayano, J. A. Taylor, S. Mukai, A. Okada, Y. Watanabe, K. Takata, and T. Fujinami, “Assessment of frequency shifts in R-R interval variability and respiration with complex demodulation,” *J. Appl. Physiol.*, vol. 77, no. 6, pp. 2879-2888, 1994.

[7] T. Kiryu, H. Yamada, M. Jimbo, and T. Bando, "Time-Varying Behavior of Motion Vectors in Vection-Induced Images in Relation to Autonomic Regulation," in *Proc. 26th Annu. Int. Conf. IEEE/EMBS*, pp. 2403-2406, San Francisco, CA, September 1-5, 2004.

[8] K. Peters, C. L. Darlington, and P. F. Smith, “The effects of repeated optokinetic stimulation on human autonomic function,” *J. Vestib. Res.*, vol. 10, no. 3, pp. 139-142, 2000.

[9] P. S. Cowings, K. H. Naifeh, W. B. Toscano, “The stability of individual patterns of autonomic responses to motion sickness stimulation,” *Aviat. Space Environ. Med.*, vol. 61, no. 5, pp. 399-405, 1990.

[10] B. J. Yates and A. D. Miller, “Physiological evidence that the vestibular system participates in autonomic and respiratory control,” *J. Vestib. Res.*, vol. 8, no. 1, pp. 17-25, 1998.

[11] J. F. Golding, M. I. Finch, and J. R. Stott, “Frequency effect of 0.35-1.0 Hz horizontal translational oscillation on motion sickness and the somatogravic illusion,” *Aviat. Space Environ. Med.*, vol. 68, no. 5, pp. 396-402, 1997.